



ALMA MATER STUDIORUM
UNIVERSITÀ DI BOLOGNA

ARCHIVIO ISTITUZIONALE
DELLA RICERCA

Alma Mater Studiorum Università di Bologna Archivio istituzionale della ricerca

Air lime mortar consolidation by nanolimes and ammonium phosphate: Compatibility, effectiveness and durability

This is the final peer-reviewed author's accepted manuscript (postprint) of the following publication:

Published Version:

Masi G., Sassoni E. (2021). Air lime mortar consolidation by nanolimes and ammonium phosphate: Compatibility, effectiveness and durability. CONSTRUCTION AND BUILDING MATERIALS, 299, 1-11 [10.1016/j.conbuildmat.2021.123999].

Availability:

This version is available at: <https://hdl.handle.net/11585/861178> since: 2022-02-19

Published:

DOI: <http://doi.org/10.1016/j.conbuildmat.2021.123999>

Terms of use:

Some rights reserved. The terms and conditions for the reuse of this version of the manuscript are specified in the publishing policy. For all terms of use and more information see the publisher's website.

This item was downloaded from IRIS Università di Bologna (<https://cris.unibo.it/>).
When citing, please refer to the published version.

(Article begins on next page)

1 **AIR LIME MORTAR CONSOLIDATION BY NANOLIMES AND AMMONIUM**
2 **PHOSPHATE: COMPATIBILITY, EFFECTIVENESS AND DURABILITY**

3
4 Giulia Masi, Enrico Sassoni*

5
6 Department of Civil, Chemical, Environmental & Materials Engineering (DICAM)
7 University of Bologna, Italy

8 * Corresponding author: enrico.sassoni2@unibo.it
9

10
11
12 **ABSTRACT**

13 In this study, a systematic comparison is presented between a commercial dispersion of
14 Ca(OH)₂ nanoparticles (so-called nanolimes) and aqueous solutions of diammonium
15 hydrogen phosphate (DAP) for consolidation of air lime mortars. The effects were
16 evaluated in terms of compatibility (composition and morphology of the new phases,
17 changes in color, porosity and water absorption), effectiveness (product uptake, dynamic
18 elastic modulus, scotch tape test) and durability (permanence of the consolidating action
19 after accelerated ageing). While both consolidants proved to be compatible, DAP solutions
20 outperformed nanolimes in terms of effectiveness and durability, especially when highly
21 concentrated DAP solutions were used.
22

23 **KEYWORDS**

24 Inorganic consolidants; Nanodispersion; Nanotechnology; Nanoparticle; Hydroxyapatite;
25 Calcium phosphate; Plaster; Render; Accelerated ageing; Scotch tape test

26 **HIGHLIGHTS**

- 27 ➤ Consolidation of lime mortars by innovative inorganic treatments was investigated
28 ➤ Nanolimes (NL) and diammonium hydrogen phosphate (DAP) were compared
29 ➤ Compatibility, effectiveness and durability after accelerated ageing were evaluated
30 ➤ Neither consolidant significantly altered color, open porosity or water absorption
31 ➤ DAP outperformed NL in terms of effectiveness and durability to accelerated ageing
32
33

34 **1. INTRODUCTION**
35

36 Consolidation of weathered air lime mortars (used as renders, plasters or bedding mortars)
37 is a complex task, especially if pigments are present, like in the case of frescoes and wall
38 paintings. For this reason, many consolidants have been proposed and tested through the
39 years, including both organic (e.g. acrylic resin [1]) and inorganic treatments (e.g. calcium
40 hydroxide [2-8], barium hydroxide [1], ethyl silicate [1,9], ammonium phosphate [10-13]).
41 Because organic treatments applied in the past decades have shown severe compatibility
42 and durability issues in the long term [14], attention has recently focused mainly on
43 inorganic treatments.

44 Among inorganic consolidants, dispersions of $\text{Ca}(\text{OH})_2$ nanoparticles (the so-called
45 nanolimes) have been extensively tested, in the light of their ideal mineralogical
46 compatibility with air lime-based substrates [15]. Indeed, $\text{Ca}(\text{OH})_2$ nanoparticles convert to
47 CaCO_3 upon carbonation, thus forming the same mineral constituting lime-based mortars
48 and carbonate stones. Nanolimes have generally shown good compatibility also in terms
49 of color change [4] (although some cases of visible whitening have been reported [6,8]), as
50 well as alterations in the pore system [8] and water transport properties [6,8]. In studies
51 evaluating lime mortars consolidation by nanolimes, a suitable consolidating effectiveness
52 has been assessed by microdrilling resistance [6,8], ultrasonic pulse velocity [5], peeling
53 resistance [8] and compressive strength [9]. However, cases of either insufficient [12] or
54 excessive strengthening [6] have also been reported. As for durability, systematic studies
55 on the salt and frost resistance of nanolime-consolidated mortars are still missing, but
56 increases in the resistance to salt weathering have been reported for nanolime-
57 consolidated stones [16-18]. However, literature studies have pointed out that nanolimes
58 cause alterations in the pore size distribution that may actually increase the crystallization
59 pressure and thus decrease the salt resistance of the substrate [18].

60 As an alternative to traditional inorganic consolidants, ammonium phosphate solutions
61 have been proposed for consolidation of carbonate substrates [19,20], also including lime
62 mortars [10-13]. The idea is to form new calcium phosphates (CaP) with binding action, by
63 treating the substrate with an aqueous solution of diammonium hydrogen phosphate (DAP,
64 $(\text{NH}_4)_2\text{HPO}_4$) [19]. While the phosphate ions necessary to form new CaP have to be
65 externally provided, the calcium ions can either come from the substrate [19] or be
66 externally supplied. In this latter case, a calcium source can be added directly into the DAP
67 solution [21] or the substrate can be pre-treated with a calcium source (such as nanolimes
68 [22-24]) before DAP application. By adding a calcium source directly into the DAP solution,
69 a significant consolidating action has been registered not only on lime-based mortars [10-
70 12] (where Ca^{2+} ion availability is high), but also on mortars based on hydraulic lime and
71 cement [11] (where Ca^{2+} ion availability is lower). The strengthening effectiveness of DAP
72 solutions applied on lime mortars has been proven by ultrasonic velocity [11-13], peeling
73 resistance [12-13] and compressive strength [11], the increase in mechanical properties
74 varying as a function of the formulation of the DAP solution. The treatment generally
75 ensures good physical-microstructural compatibility, because changes in pore size
76 distribution and water transport properties are minor [11-13]. In terms of aesthetic
77 compatibility, negligible color alterations have been found on lime-based mortars (initially
78 white), whereas some whitening was observed when highly concentrated DAP solutions
79 were used on mortars containing brick dust (initially pink), hydraulic lime (initially brown) or
80 cement (initially gray) [11]. As for durability, encouraging results have been obtained on
81 porous stones, in terms of resistance to salt crystallization [23,25,26] and freezing-thawing
82 cycles [25,26], but systematic studies are still missing in the specific case of lime mortars.

83 Therefore, the aim of the present study was to perform a systematic comparison between
84 nanolimes and ammonium phosphate applied onto lime mortars. A few studies comparing
85 the performance of these two consolidants have been reported in the literature on stones
86 [24,26,27] and mortars [12], but in the present study all the main requirements of a

87 consolidant (namely, compatibility, effectiveness and durability) were systematically
88 evaluated on lime mortars for the first time. In this work, the consolidants were tested on
89 mortar samples applied onto a brick substrate, to resemble the situation of plasters and
90 renders that were traditionally applied onto brick masonry. However, the intended
91 application of these products also includes consolidation of bedding mortars and
92 decorative mortars often used to imitate natural stones (the so-called “artificial stones”).

93

94 **2. MATERIALS AND METHODS**

95

96 **2.1. Specimens**

97 Multilayer specimens, composed of a layer of air lime mortar over a brick substrate, were
98 used for the tests. It is noteworthy that, in the present case, a single mortar layer was
99 applied onto the substrate, whereas historic plasters and renders were usually composed
100 of multiple layers with different composition and porosity.

101 First, slabs ($5 \times 5 \times 1 \text{ cm}^3$) were sawn from a single brick, to ensure that all the brick
102 substrates have the same porosity and, hence, the same behavior for all the specimens.
103 The brick slabs were let saturate with water for 24 hours before applying the mortar layer,
104 to prevent bricks from absorbing water from the mortar, which would alter the water to
105 binder ratio and the porosity of the mortar [28]. A 1 cm-thick layer of lime mortar, prepared
106 as described in the following, was then applied onto the brick slabs.

107 The lime mortar was prepared using hydrated lime by Colacem, Italy (CL 70-S according
108 to EN 459-1:2015) and calcareous sand ($\text{CaCO}_3 = 95 \pm 1.5 \text{ wt}\%$, maximum particle size of
109 4 mm). A binder-to-aggregate ratio of 1:2 v/v (0.41 w/w) and a water-to-binder ratio of 1:1
110 v/v (0.45 w/w) were used. The mortar was mixed in a Hobart mixer, then poured onto the
111 brick slabs inside plastic molds and finally manually leveled out. The sandwich specimens
112 ($5 \times 5 \text{ cm}^2$ cross section, composed of 1 cm of mortar over 1 cm of brick) were then
113 immediately demolded and left to cure in a climatic chamber ($\text{RH} = 90 \pm 2\%$, $T = 21 \pm 2$
114 $^\circ\text{C}$) for 4 months. The adopted RH value was selected considering that, in the case of
115 $\text{Ca}(\text{OH})_2$ nanoparticles, faster and more thorough carbonation was systematically
116 observed for RH increasing from 33 % up to 95 % [15]. After curing for 4 months in these
117 conditions, carbonation of the lime mortar specimens could be considered as complete,
118 since no residual portlandite band was detected by FT-IR performed on the lime mortar.

119

120 **2.2. Consolidants**

121 A commercial product based on nanolimes and two different formulations of the DAP
122 treatment were tested, so that in total 4 conditions were considered:

123 1) Untreated reference (labelled “UT”).

124 2) Nanolimes (labelled “NL”). The commercial product Nanorestore Plus® Ethanol 5 by
125 CTS Srl (Italy), consisting in a dispersion of calcium hydroxide nanoparticles in

126 ethanol with a concentration of 5 g/L, was used. As recommended by the producer
127 to prevent whitening, a sheet of Japanese paper was first applied onto the surface
128 to be treated (i.e. the 5×5 cm² face of the mortar specimens) and then the
129 nanodispersion was applied by brushing 10 times, waiting for the product to be
130 absorbed between subsequent brush strokes. As recommended in the product's
131 technical data sheet, immediately at the end of the brush application, a poultice of
132 cellulose pulp imbibed with deionized water (1:4 weight ratio) was applied over the
133 sheet of Japanese paper, to favor carbonation and to prevent white haze formation.
134 The presence of water favors carbonation because atmospheric CO₂ and Ca(OH)₂
135 both need to dissolve in water (in bulk or adsorbed onto the nanoparticles) for the
136 carbonation reaction to take place [15]. The poultice was left to dry in contact with
137 the specimens for 3 days and finally removed.

138 3) Aqueous solution containing 1 M DAP + 1 mM CaCl₂ (labelled "D1"). This
139 formulation, first proposed for marble protection [21], was here selected as it has
140 shown also significant consolidating effectiveness on different types of substrate
141 [12,20,29]. The addition of CaCl₂ as a calcium source has the effect of promoting
142 and accelerating formation of new CaP [21], also on substrates where the
143 availability of calcium ions from the substrate would be limited [11]. The solution
144 (prepared using chemicals supplied by Sigma-Aldrich) was applied by brushing 10
145 times over the 5×5 cm² face of the mortar specimens. Then, the specimens were
146 wrapped in a plastic film to prevent evaporation of the consolidating solution. After
147 24 hours, the specimens were unwrapped, rinsed with deionized water and left to
148 dry at room temperature until constant weight.

149 4) Aqueous solution containing 3 M DAP (labelled "D3"). This alternative formulation of
150 the DAP treatment was selected because it has shown a significant consolidating
151 effectiveness, even on highly deteriorated substrates, thanks to the high
152 concentration of phosphate ions available to form new CaP [13,20,30,31]. The
153 solution was applied by brushing 10 times over the 5×5 cm² face of the mortar
154 specimens. Similar to the case of the D1 treatment, after application of the DAP
155 solution the specimens were wrapped in a plastic film for 24 hours, then the film
156 was removed, the specimens rinsed with water and dried at room temperature until
157 constant weight. Finally, to ensure that no unreacted DAP remain in the mortar, a
158 poultice of cellulose pulp and limewater (i.e. a saturated solution of calcium
159 hydroxide, 1.7 g/L, supplied by Sigma-Aldrich) with a 1:4 weight ratio was applied
160 onto the treated surface, interposing a sheet of Japanese paper to avoid sticking.
161 The specimens were again wrapped in a plastic film for 24 hours (so that calcium
162 ions contained in limewater could penetrate into the mortar and react with possible
163 unreacted DAP [31]), then the specimens were unwrapped and finally left to dry
164 while still covered with the poultice (so that all the soluble fractions could be
165 extracted from the mortar and transported into the poultice [31]).

166 Before testing, all the specimens were left to cure for 4 weeks in a climatic chamber (RH =
167 90 ± 2%, T = 21 ± 2 °C). The RH value was selected to promote nanolime carbonation, for
168 the reasons discussed above [15]. The duration was selected as the nanolime technical
169 data sheet recommends curing for 2-4 weeks, while curing for a much shorter time would

170 be sufficient for the DAP treatments (namely 24 hours for D1 and about 1 week for D3,
171 which also involves drying and application of limewater).

172

173 **2.3. Characterization**

174 **2.3.1. Compatibility**

175 Composition and morphology of the new phases. The composition of the new phases was
176 investigated by Fourier Transform Infrared Spectrometry (FT-IR), on powdered samples
177 obtained from the specimen surface using a spatula. A Perkin Elmer Spectrum Two
178 instrument (ATR mode, 2000-500 cm^{-1} range, spectral resolution 2 cm^{-1} , 32 scans, data
179 interval 1 cm^{-1}) was used. To allow for a qualitative comparison between the amounts of
180 new phases formed after treatment, the FT-IR spectra were normalized with respect to the
181 calcite band at 872 cm^{-1} . The morphology of the new phases was analyzed by scanning
182 electron microscopy (SEM), using a Field Emission Gun (FEG) instrument (Tescan Mira3)
183 equipped with energy dispersive spectrometry (EDS, Bruker probe). Two types of samples
184 were observed by FEG-SEM: fracture surfaces and polished cross sections. Fracture
185 surfaces were observed on samples ($\sim 1 \text{ cm}^3$) collected by chisel after mechanical testing
186 (cf. § 2.3.2). Cross sections were prepared by encapsulating other samples (containing the
187 original treated surface) in epoxy resin and then polishing the encapsulated samples to
188 expose the cross section. All the FEG-SEM samples were made conductive by
189 evaporation of graphite before observation (Quorum Q150R ES+ coater).

190 Aesthetic compatibility. The color difference after consolidation was evaluated by
191 measuring the CIE Lab color parameters (L^* = black-white, a^* = green-red, b^* = blue-
192 yellow) of untreated and treated specimens, using a NH310 colorimeter. For each
193 condition, three specimens were analyzed and, for each specimen, colorimetric
194 measurements were performed in three different spots. The average CIE Lab color
195 parameters were then calculated for each condition and the resulting color difference ΔE^*
196 between treated and untreated samples was determined as $\Delta E^* = (\Delta a^{*2} + \Delta b^{*2} + \Delta c^{*2})^{1/2}$.

197 Physical compatibility. The alterations in open porosity and pore size distribution were
198 evaluated by mercury intrusion porosimetry (MIP) using a Pascal 140 and 240 instrument
199 (minimum pressure 0.0125 MPa, maximum pressure 200 MPa). The MIP samples (~ 1
200 cm^3) were collected by chisel after mechanical testing (cf. § 2.3.2). The alteration in water
201 sorptivity was determined according to the European Standard EN 15801 [32]. Water was
202 let penetrate the samples through the $5 \times 5 \text{ cm}^2$ mortar face (hence with the brick slab
203 upwards), until saturation was reached after about 6 hours. Three replicates were tested
204 for each condition.

205

206 **2.3.2. Effectiveness**

207 Product uptake. The amount of liquid consolidant absorbed by the specimens was
208 determined by weighing the specimens before and right after the consolidant application.

209 Dynamic elastic modulus (E_d). The increase in cohesion after consolidation was evaluated
210 by determining the E_d on each specimen, before and after treatment, according to the

211 formula $E_d = \rho \times UPV^2$, where ρ is the density and UPV is the ultrasonic pulse velocity. UPV
212 can be measured non-destructively and has been shown to be strongly correlated with
213 porosity and mechanical properties in natural stones (especially marbles [33]), so UPV and
214 E_d are commonly used to assess the consolidation effectiveness also on lime mortars
215 [5,11-13]. The UPV was measured using a Pundit instrument with 55 kHz transducers. To
216 ensure that the ultrasonic pulse travel only through the 1-cm thick mortar layer (and not
217 through the adjacent 1-cm thick brick layer), 0.8×5 cm² rubber pieces were used between
218 the transducers and the specimens, thus also improving the contact between the two. For
219 each condition, three replicate specimens were tested.

220 Scotch tape test (STT). An indication about the ability of the consolidants to increase the
221 mortar resistance to material loss was obtained by STT [34]. The test was performed by
222 first applying a piece of adhesive tape onto the specimens and making it adhere uniformly.
223 The scotch tape measured 6×2.5 cm², equivalent to half of the mortar face (5×5 cm²), plus
224 an extra 1 cm to allow for the tape removal. The tape was then manually removed, always
225 adopting the same speed and angle of removal. The amount of mortar detached from the
226 specimen and attached to the scotch tape was determined by weighing the tape before
227 and after the test. To evaluate the consistency with depth of the consolidating action, on
228 each specimen the STT was repeated 10 times in the same position. For each condition,
229 three replicate specimens were tested.

230

231 **2.3.3. Durability**

232 The permanence of the consolidating action after accelerated ageing was assessed by
233 subjecting the specimens to freezing-thawing cycles and then repeating the
234 characterization tests described above. Freezing-thawing cycles were preferred over salt
235 crystallization cycles because both deterioration processes cause stress in the pores and
236 a decrease in mechanical properties, but salt crystallization cycles also induce
237 contamination of the specimens and formation of efflorescence, which would make it
238 impossible to repeat the STT after ageing. The freezing-thawing cycles were performed by
239 partly modifying the European Standard EN 12371 [35]: after being preliminarily saturated
240 with deionized water by immersion for 3 days, the specimens were subjected to cycles of
241 freezing at -20±2 °C for 2 h, followed by thawing in water at +20±2 °C for 2 h. After 10
242 cycles, the specimens were dried in an oven at 50 °C for 3 days. The effects of
243 accelerated ageing were then assessed by measuring the weight loss and by repeating
244 SEM observation, E_d measurement and STT after the cycles, following the same
245 procedures described above.

246

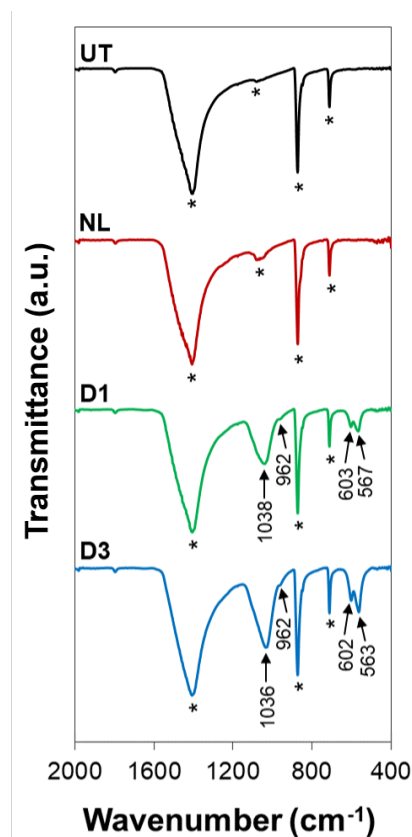
247 **3. RESULTS AND DISCUSSION**

248

249 **3.3.1. Compatibility**

250 In terms of composition of the new phases, nanolimes and DAP can both be considered as
251 suitably compatible. Indeed, nanolimes caused formation of calcite (i.e. the same mineral
252 constituting the substrate), while no metastable CaCO₃ minerals (e.g. vaterite or aragonite,
253 which can result from nanolime carbonation [15]) were detected by FT-IR (Figure 1). In the

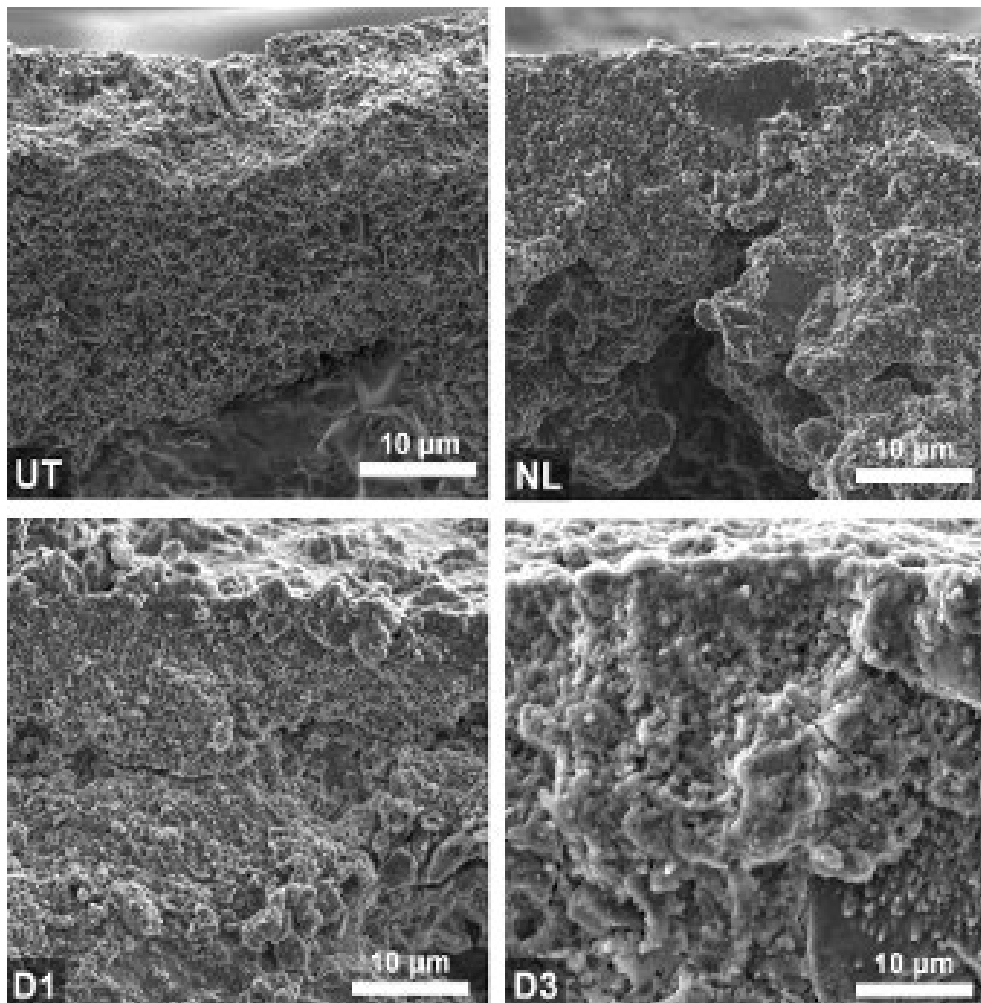
254 case of the DAP-based treatments, FT-IR spectra suggest that, in the “D1” sample,
 255 octacalcium phosphate (OCP, $\text{Ca}_8(\text{HPO}_4)_2(\text{PO}_4)_4 \cdot 5\text{H}_2\text{O}$) was formed (OCP having bands
 256 at 1038, 961, 602, 560 cm^{-1} [36]). In the D3 sample, hydroxyapatite (HAP,
 257 $\text{Ca}_{10}(\text{PO}_4)_6(\text{OH})_2$) seems to have formed (HAP having bands at 1031, 962, 604, 563 cm^{-1}
 258 [36]), although the presence of OCP cannot be completely excluded. HAP, being the least
 259 soluble CaP at $\text{pH} > 4$, is the ideal mineral to form, but OCP is not undesirable, considering
 260 that it is significantly less soluble than calcite [21]. The present findings are consistent with
 261 previous results reported in the literature, pointing out that OCP formation is favored by
 262 addition of CaCl_2 to the DAP solution (like in treatment “D1”), while HAP is formed when
 263 only DAP is used (like in treatment “D3”) [21]. In the case of the “D3” sample, the increase
 264 in the height of the calcite band at 712 cm^{-1} suggests that carbonate ions (coming from the
 265 mortar substrate and/or from the atmosphere) were likely incorporated into the HAP lattice,
 266 thus leading to formation of carbonated HAP [19]. However, phase identification is very
 267 challenging, because of the similarity in the crystal structure of different CaP minerals, so a
 268 multiplicity of analytical techniques (ideally also including synchrotron analyses) would be
 269 necessary for a conclusive phase identification [37,38]. Notably, the amount of new CaP
 270 phases formed after the “D3” treatment appears considerably higher than that formed
 271 using the “D1” formulation, in agreement with previous results [30]. HAP and OCP can be
 272 regarded as fully compatible minerals, considering that (although not originally present in
 273 lime mortars or carbonate stones) they have been found in natural patinas formed through
 274 the centuries over historic monuments [39]. Such patinas do not cause deterioration of the
 275 substrate, but on the contrary exert a significant protective action, so that during cleaning
 276 interventions it is nowadays usually recommended that such patinas be preserved.



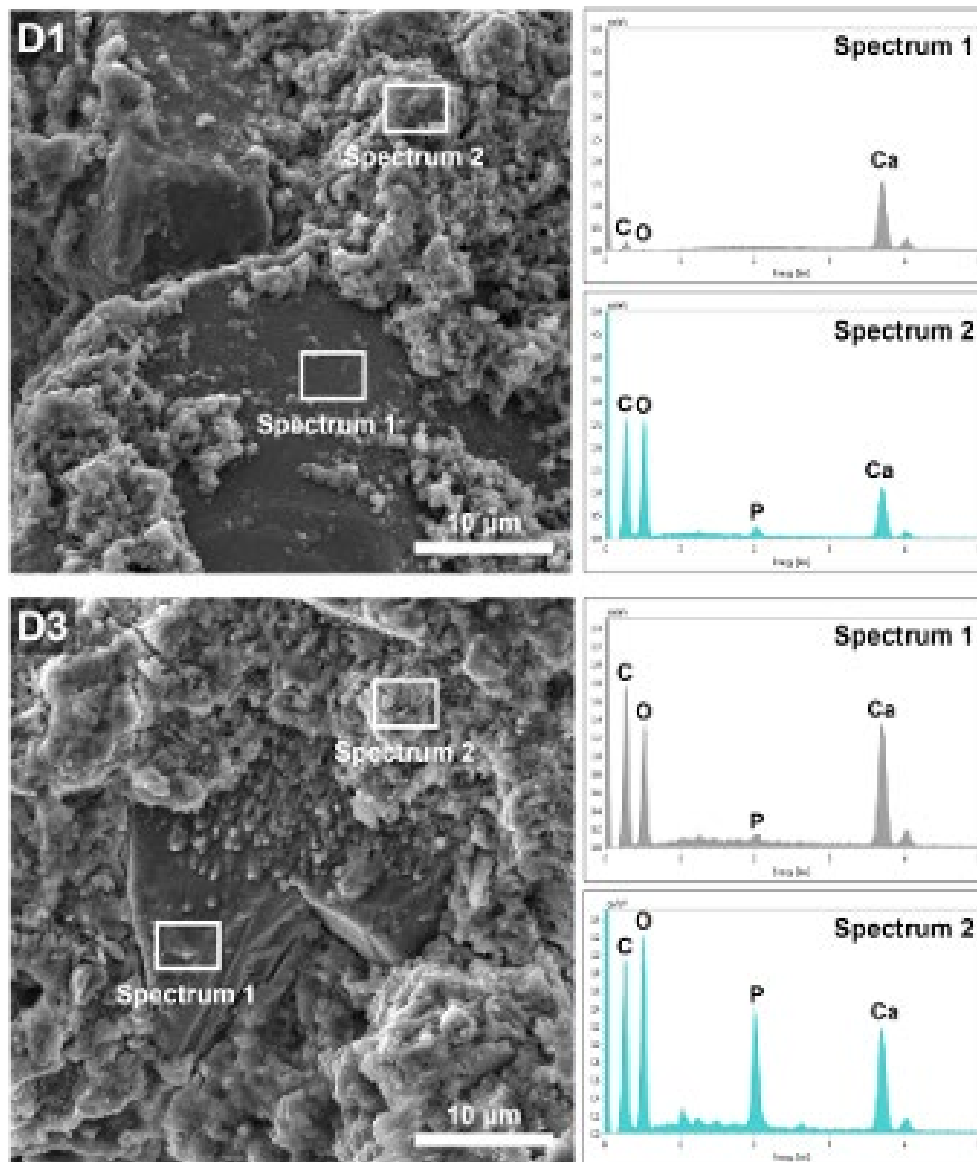
277
 278 **Figure 1.** FT-IR spectra of untreated and treated specimens (bands attributed to the substrate are
 279 marked with a *, while the position of new bands is reported).

280 SEM observation of fracture surfaces (Figure 2 and Figure 3) and polished cross sections
281 (Figure 4) revealed that in no case was a clear superficial crust formed after treatment.
282 While in the case of nanolimes the elemental composition of the substrate and the
283 consolidant is the same, so that the consolidant presence cannot be traced by chemical
284 analysis, in the case of the DAP-treatments EDS provided useful information about the
285 penetration depth. Starting from the treated surface, phosphorus was detected through all
286 the mortar thickness (1 cm), the signal being higher in the “D3” sample than in the “D1”
287 one (Figure 3). This further confirmed that a higher amount of new CaP phases was
288 formed after the “D3” treatment, in agreement with the FT-IR results. The high penetration
289 depth registered in the present case (at least 1 cm) is consistent with previous results on
290 lime mortars, as DAP solutions have been reported to penetrate from at least 1 cm [13] up
291 to 4 cm [11] from the treated surface. In the case of nanolimes, no clear indication about
292 the penetration depth could be obtained by EDS, nor was morphology observation
293 sufficient to derive conclusive information. According to the literature, depending on the
294 porosity of the substrate, penetration down to 4 cm from the treated surface has been
295 reported [40], but nanoparticle transport back to the surface during drying has been
296 observed, which may be responsible for particle accumulation near the surface [40].

297

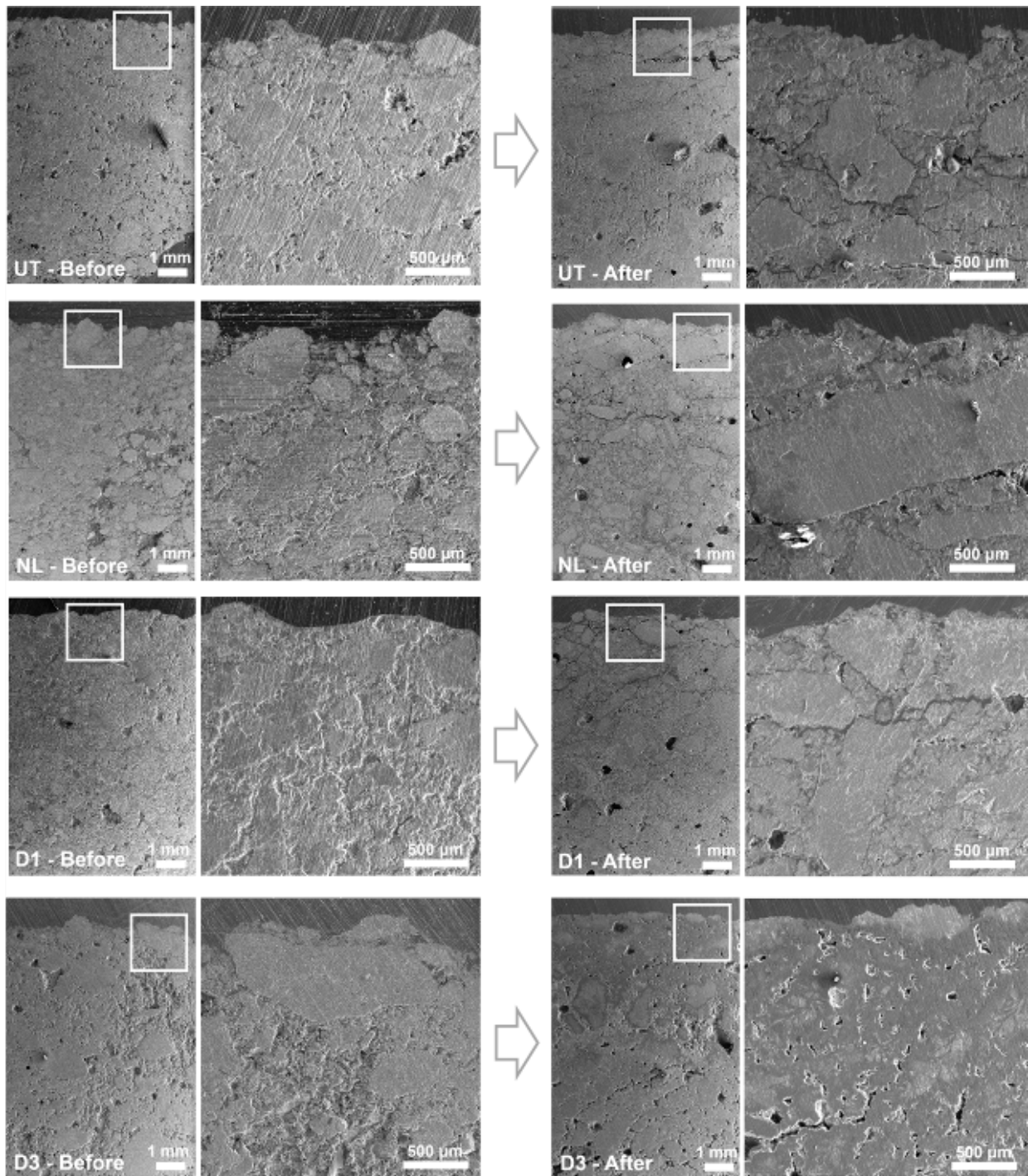


298 **Figure 2.** SEM images of fracture surfaces of untreated and treated samples, before accelerated
299 ageing by freezing-thawing cycles.
300
301



302
 303 **Figure 3.** SEM images and EDS spectra of samples treated by DAP (treated surface in the upper
 304 part).
 305

306 The new consolidating phases were responsible for some alterations in the mortar
 307 aesthetic appearance (Table 1), but the resulting color change can be considered as
 308 always acceptable (Figure 5). The “NL” and “D1” treatments caused color changes ($\Delta E^* =$
 309 1.2 and 2.2, respectively) even below the visibility limit ($\Delta E^* = 2.3$ [41]). “D3” caused a
 310 higher color change ($\Delta E^* = 4.3$), mostly owing to a decrease in lightness and a shift
 311 towards blue (Table 1), but the color alteration was anyway below the common
 312 acceptability limit ($\Delta E^* = 5$ [42]). However, in view of the possible application to colored
 313 plasters and renders, the color alteration induced by the “D3” treatment should be
 314 specifically investigated case by case. All things considered, in the present study none of
 315 the consolidants gave rise to aesthetic compatibility issues.



316

317

318

319

320

321

322

323

Figure 4. SEM images of polished cross sections of untreated and treated samples, before (left) and after (right) accelerated ageing by freezing-thawing cycles.

Table 1. Color parameters (L^* = black-white, a^* = green-red, b^* = blue-yellow) on untreated and treated specimens and resulting variations ΔL^* , Δa^* , Δb^* , ΔE^* (L^* , a^* , b^* are averages for 9 measurements).

	L^*	a^*	b^*	ΔL^*	Δa^*	Δb^*	ΔE^*
UT	94.0 ± 0.2	-0.5 ± 0.0	1.8 ± 0.1	-	-	-	-
NL	92.9 ± 0.5	-0.4 ± 0.0	2.4 ± 0.2	-1.1	0.1	0.6	1.2
D1	92.1 ± 0.5	-0.5 ± 0.0	2.7 ± 0.2	-1.9	0.0	1.0	2.2
D3	91.2 ± 0.5	-0.4 ± 0.1	5.0 ± 0.8	-2.7	0.1	3.3	4.3

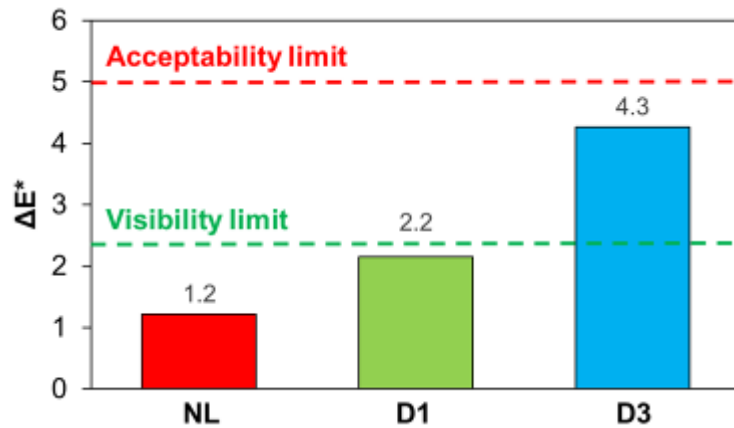
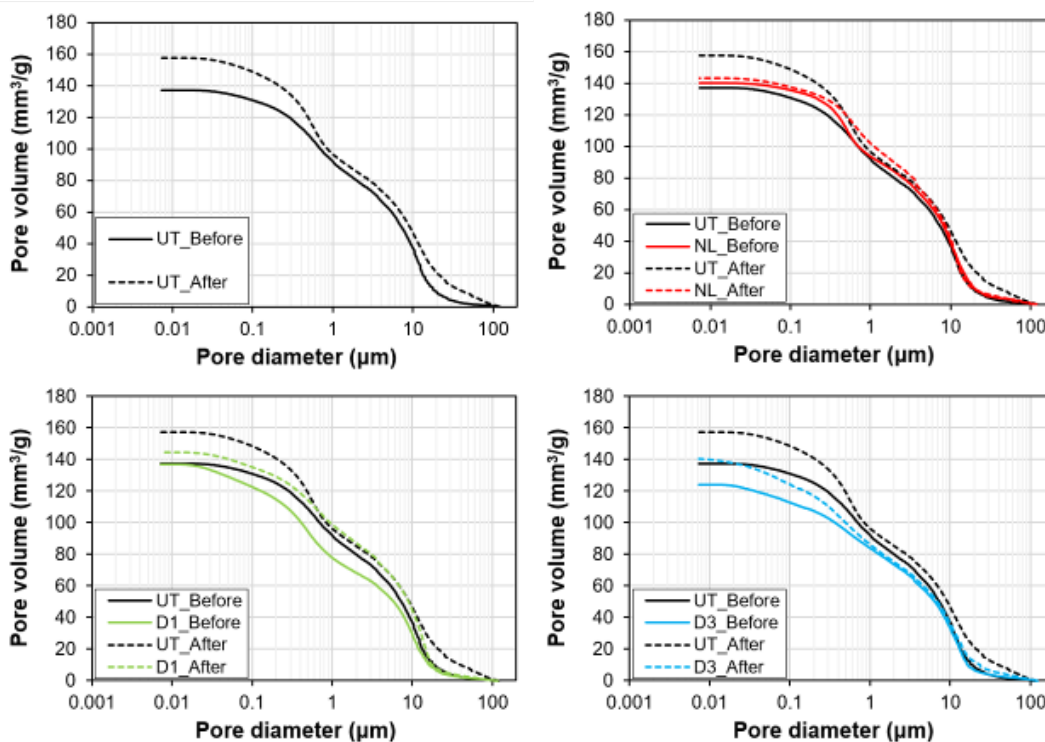


Figure 5. Color change after treatment by the various consolidants.

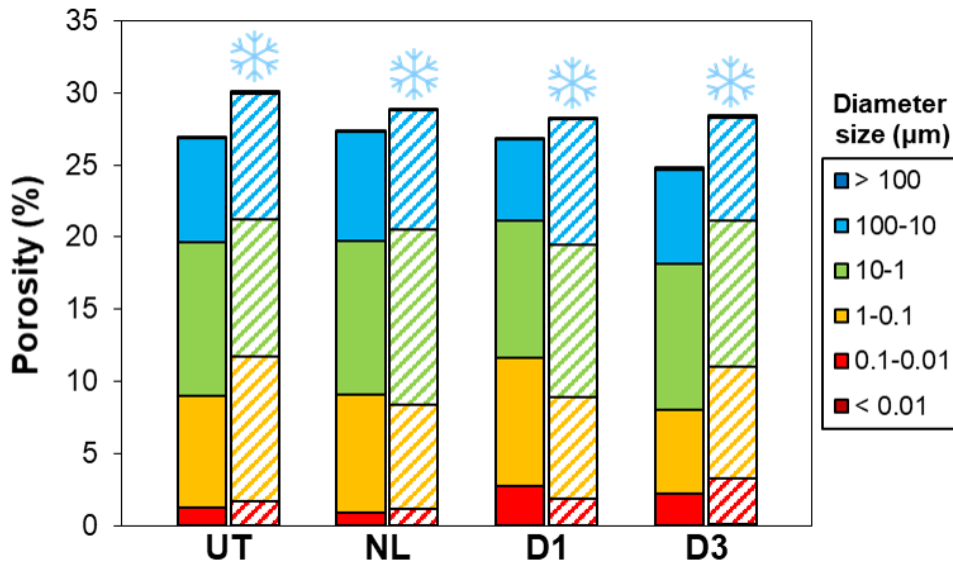
324
325
326
327
328
329
330
331
332
333
334
335
336
337
338
339

The new consolidating phases also caused some limited alterations in the mortar pore system, as shown in Figure 6 (solid lines) and Figure 7 (solid bars). In terms of total open porosity (OP), compared to the untreated reference (OP = 26.9%), the “NL” and “D1” treatments caused negligible changes, while the “D3” treatment caused the most pronounced alteration, which was however very limited (OP = 24.7%). In terms of pore size distribution (Figure 7), the “NL” treatment caused basically no alteration, while “D1” and “D3” caused a slight decrease in the amount of bigger pores and a corresponding increase in the amount of smaller pores. This is the effect of the new CaP formation, which partly occluded the bigger pores, thus apparently forming new smaller pores. The limited effect of the DAP-treatments on the pore system, mainly consisting in a slight shift in pore size distribution towards smaller pores, is consistent with previous results on stones [43] and mortars [11].



340
341
342

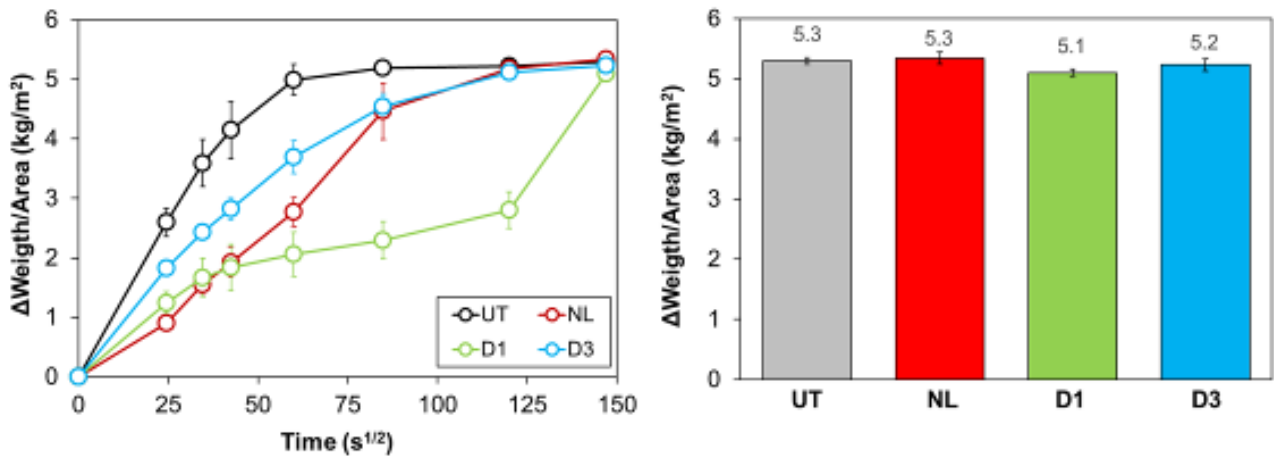
Figure 6. Cumulative pore volume of untreated and treated samples, before (solid lines) and after (dotted lines) accelerated ageing by freezing-thawing cycles.



343
 344 **Figure 7.** Pore size distribution of untreated and treated samples, before (solid bars) and after
 345 (hatched bars) accelerated ageing by freezing-thawing cycles (indicated by the frost symbol).

346
 347 Consistent with the limited changes in the pore system, none of the consolidants caused
 348 significant alterations in water transport properties (Figure 8). Some reduction in the rate of
 349 water sorption was registered in all the samples (because water is absorbed more slowly
 350 in smaller pores and the treatments caused a slight shift of the pore size distribution
 351 towards smaller pores, Figure 6), but the final absorption corresponded to full saturation
 352 for all the conditions. It is noteworthy that the “D1” samples apparently experienced some
 353 reduction in sorptivity in the middle part of the test (green curve between about 50 and 125
 354 $s^{1/2}$). Considering that the “D1” samples experienced a less pronounced modification in
 355 pore size distribution than the “D3” ones and that “D3” samples exhibited a limited
 356 alteration in water sorptivity, the slowing down of water absorption registered for the “D1”
 357 samples is likely to be ascribed to the experimental conditions during the test. In fact, the
 358 water level has to be manually maintained constant during the test by periodically refilling
 359 water in the container with the samples. Most likely, the apparent reduction in water
 360 sorptivity of the “D1” samples was due to a decrease in the water level in the middle part of
 361 the test. A limited alteration in water absorption can be regarded as positive, considering
 362 that conservation treatments that cause a strong alteration in water transport properties
 363 (e.g. hydrophobic treatments, also including ethyl silicate) may give rise to compatibility
 364 issues if a water source is present behind the consolidated layer, which acts as a barrier
 365 preventing water from exiting the consolidated material [44].

366



367
368 **Figure 8.** Water sorptivity (left) and total water absorption (right) of untreated and treated
369 specimens.

370

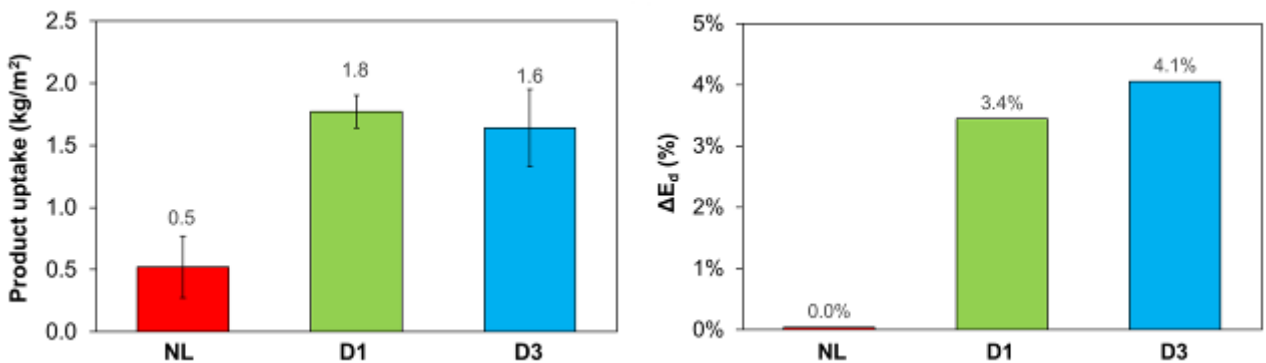
371

372

2.3.4. Effectiveness

373 The amount of liquid consolidants absorbed by the specimens is reported in Figure 9. In
374 the case of the DAP-treatments, the amounts found in this study for lime mortars (1.6-1.8
375 kg/m²) are in good agreement with the values previously reported for porous limestone
376 (1.4-1.5 kg/m² [43]), the difference being ascribable to the specific properties of two
377 substrates. In the case of nanolimes, the product uptake (0.5 kg/m²) was lower compared
378 to the DAP-treatments, which can be explained considering the different concentrations of
379 the consolidants (5 g/L for “NL”, 132 g/L for “D1” and 396 g/L for “D3”) and the different
380 volatility of the solvents (ethanol, having vapor pressure of 5.8 kPa, for “NL”; water, having
381 vapor pressure of 2.3 kPa, for “D1” and “D3”).

382



383
384 **Figure 9.** Product uptake (left) and percentage UPV increase (right) after treatment by the various
385 consolidants

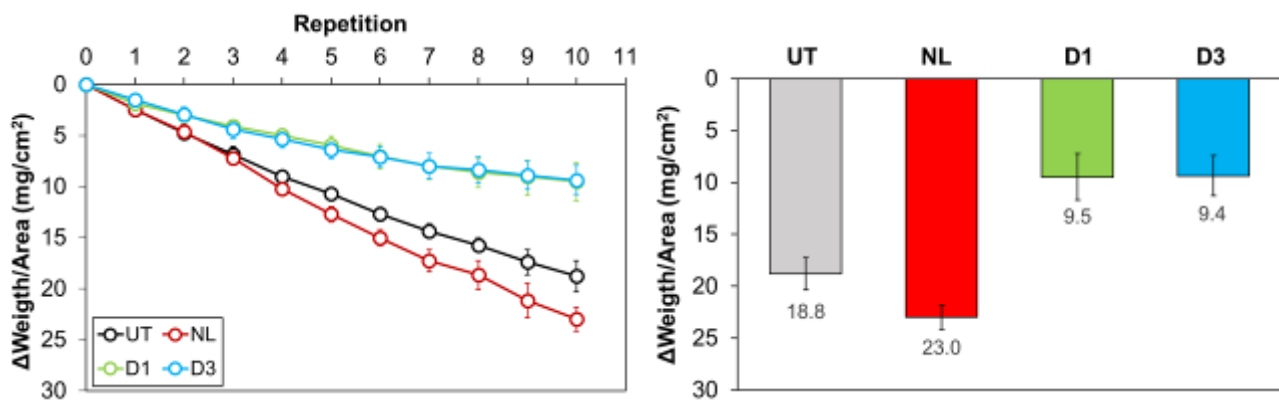
386

387 After curing, the liquid consolidants formed new CaP binding phases that caused the
388 increases in E_d reported in Figure 9 and the decreases in materials loss after STT reported
389 in Figure 10.

390 The E_d increases were actually modest (reaching +4.1% for “D3”), which was unexpected
391 considering that E_d increases up to +75% [11] and +100% [13] had been obtained in

392 previous studies on lime mortar consolidation by similar DAP formulations, while UPV
 393 increases up to +10% had been reported for mortars treated with nanolimes [5]. A first
 394 reason for such low E_d increases may be that, while in marbles UPV measurements are
 395 able to effectively detect the formation of new binding phases in intergranular fissures, in
 396 highly porous materials like mortars the bridging effect of the new phases leads to UPV
 397 increases much less evident, because the overall porosity of the material is basically
 398 unchanged (Figure 6). A second reason for the modest E_d increases may be the specific
 399 experimental set-up adopted in this study (i.e. UPV measurements across mortar layers
 400 that are attached to brick substrates), which may be altered by the presence of the brick
 401 layer. However, in a previous study where the same experimental set-up had been used
 402 for a different type of substrate (lime mortars containing siliceous aggregates, instead of
 403 calcareous ones), higher improvements (Δ UPV of +5% for “NL”, +17% for DAP) had been
 404 recorded [12].

405



406

407

Figure 10. Progressive (left) and cumulative (right) material loss after STT on untreated and treated specimens.

408

409

410 An indication of the actual consolidating ability of the various treatments investigated in
 411 this study was obtained by STT. As illustrated in Figure 10, the scarce effectiveness of
 412 nanolimes, already suggested by ultrasonic measurements ($\Delta E_d = 0\%$), was confirmed, as
 413 the cumulative material loss after 10 STT was substantially the same for the “NL” and the
 414 “UT” specimens (actually, slightly higher for the former). Even though no clear formation of
 415 a surface crust was observed by SEM (Figure 2 and Figure 4), still the lack of
 416 consolidating effectiveness is likely due to scarce formation of new binding phases deep in
 417 the mortar, resulting in unchanged cohesion after consolidation. The higher weight loss
 418 apparently exhibited by the “NL” specimens, compared to the “UT” ones, may actually be
 419 due to the easy removal of newly formed calcite crystals deposited mainly near the tested
 420 surface. In the case of the DAP-treatments, significant decreases in material loss after
 421 STT were registered (about -50% for both “D1” and “D3”, Figure 9). Such improvements in
 422 resistance to STT are higher than those reported in a previous study, where alternative
 423 formulations of the DAP treatment had been tested on lime mortars (decreases in material
 424 loss by STT by 35%) [13]. In the present study, the effects of “D1” and “D3” appear similar
 425 based on STT results, whereas a higher improvement for “D3” was suggested by E_d
 426 measurements (Figure 8).

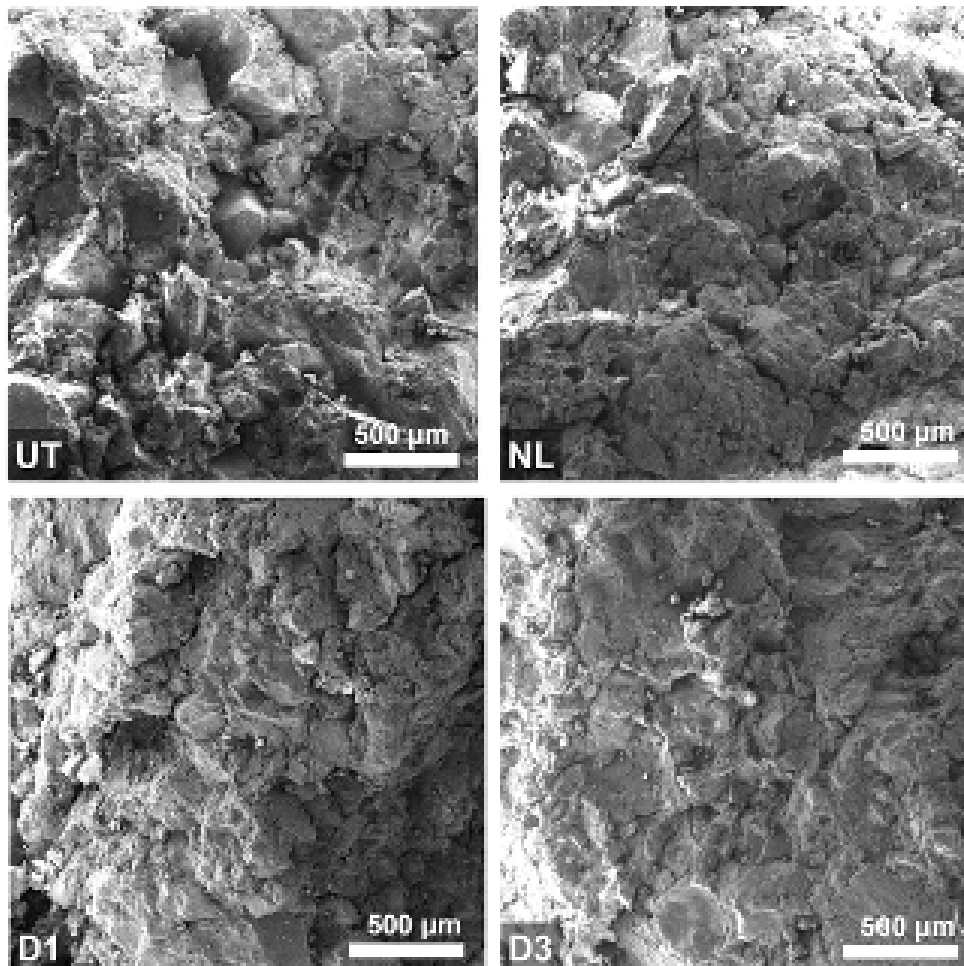
427 All things considered, the consolidating effectiveness of the various treatments increased
428 in the order: UT \approx NL < D1 < D3. A confirmation of such trend was further obtained by the
429 results of the durability tests, described in the following.

430

431 **2.3.5. Durability**

432 Accelerated ageing by freezing-thawing cycles had a dramatic effect on untreated mortar,
433 which underwent formation of new microcracks clearly visible by SEM (Figure 4 and Figure
434 11), resulting in increased open porosity and pore size (Figure 7). This led to a significant
435 loss in cohesion after ageing, evidenced by the high weight loss (-1.1%) and high E_d
436 decrease (-52.6%) (Figure 12) after the cycles, as well as dramatic material loss when the
437 STT was repeated (Figure 13). After the freezing-thawing cycles, the cumulative material
438 loss by STT reached 338.5 mg/cm², hence almost 20 times more than before accelerated
439 ageing (18.8 mg/cm², Figure 10).

440



441

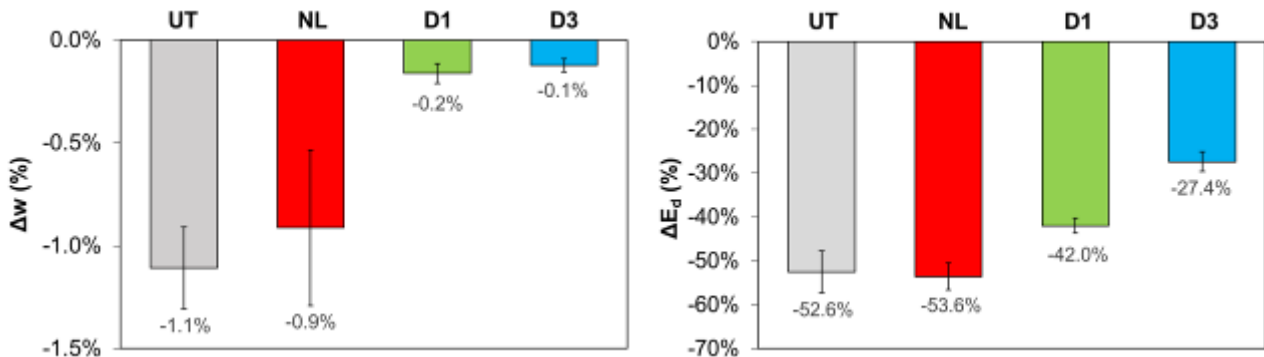
442 **Figure 11.** SEM images of fracture surfaces of untreated and treated samples, after accelerated
443 ageing by freezing-thawing cycles.

444

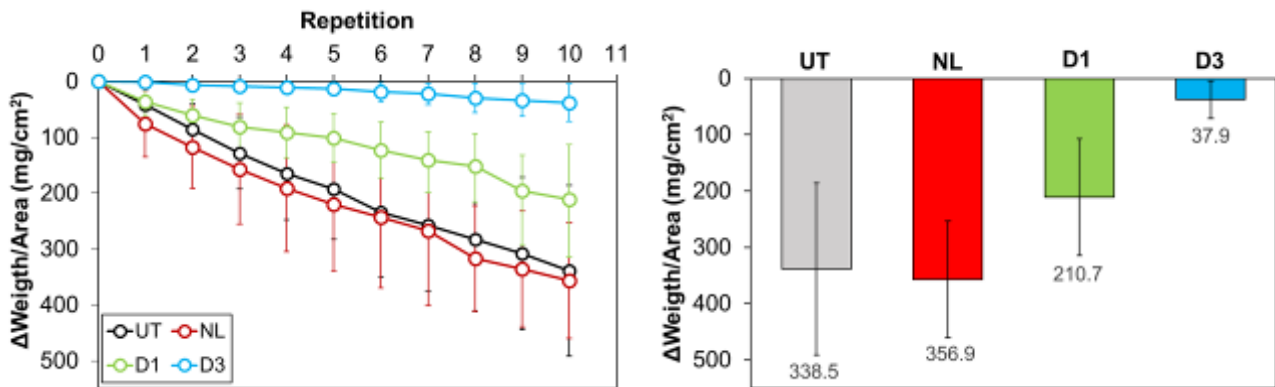
445

446 Specimens treated by nanolimes exhibited similar cracking (Figure 4 and Figure 11) and
447 alterations in open porosity and pore size distribution (Figure 6 and Figure 7) as the

448 untreated reference. Accordingly, comparable weight loss (-0.9%) and E_d decrease (-
 449 53.6%) were registered (Figure 12). Consistently, also the STT pointed out a similar
 450 material loss for the two conditions (actually, slightly higher for “NL” than “UT”, Figure 12),
 451 indicating that no significant consolidation was obtained by nanolimes.



452
 453 **Figure 12.** Weight loss (left) and percentage UPV loss (right) of untreated and treated specimens
 454 after accelerated ageing by freezing-thawing cycles.
 455



456
 457 **Figure 13.** Progressive (left) and cumulative (right) material loss after STT on untreated and
 458 treated specimens after accelerated ageing by freezing-thawing cycles.
 459

460 In the case of the DAP-treatments, less pronounced cracking (Figure 4 and Figure 11) and
 461 formation of new voids (Figure 6 and Figure 7) were registered after the freezing-thawing
 462 cycles, compared to the “UT” and “NL” conditions. Both DAP treatments also allowed to
 463 significantly reduce the weight loss after the freezing-thawing cycles (-0.2% for “D1” and -
 464 0.2% for “D3”, compared to -1.1% for the “UT” reference, Figure 12). The “D3” treatment
 465 proved to be the most effective in reducing damage caused by the ageing cycles, in
 466 agreement with the results obtained right after consolidation. Indeed, this formulation
 467 caused the lowest E_d decrease (-27.4%, compared to -52.6% for “UT”, Figure 11) and the
 468 lowest material loss by STT (-37.9 mg/cm², compared to -338.5%, Figure 12).

469 All things considered, the durability tests confirmed and better elucidated the trend in
 470 consolidating effectiveness of the various treatments, whose performance improved in the
 471 following order: UT \approx NL < D1 < D3.

472
 473
 474

475 4. CONCLUSIONS

476

477 The present study aimed at evaluating the compatibility, effectiveness and durability of two
478 different consolidating treatments for lime mortars, namely nanolimes (“NL”) and DAP
479 solutions, tested in two formulations (“D1”, less concentrated, and “D3”, more
480 concentrated). Based on the obtained results, the following conclusions can be derived:

481 ➤ the “NL” treatment proved to be fully compatible (invisible color change and negligible
482 alteration in open porosity and water absorption), but demonstrated very limited
483 consolidating effectiveness (no decrease in material loss by scotch tape test, STT).
484 When NL-treated specimens were subjected to accelerated ageing by freezing-thawing
485 cycles, the “NL” treatment was not able to provide a significant benefit (no reduction in
486 material loss when STT was repeated after the cycles).

487 ➤ the DAP-based treatments, especially the more concentrated one “D3”, were effective
488 in decreasing the material loss by STT (-50%, compared to the untreated reference)
489 and maintained the consolidating ability also after the freezing-thawing cycles (in the
490 case of “D3”, after accelerated ageing material loss was reduced by 10 times,
491 compared to the untreated reference). Such consolidating effectiveness and durability
492 to accelerated ageing were obtained without significant chromatic alterations (invisible
493 color change for “D1”, visible but acceptable for “D3”) and without significant alterations
494 in open porosity and water absorption.

495 The results obtained in this study confirm the potential of DAP solutions for consolidation
496 of lime-based mortars, plaster and renders. Compared to nanolimes, DAP solutions
497 proved to be more effective, also after accelerated ageing, with the advantage that the
498 DAP treatment only requires curing for 24 hours, while carbonation of nanolimes requires
499 up to 4 weeks. As the next step, future research will be dedicated to investigate the effects
500 of DAP solutions when applied onto colored plasters and renders (e.g. frescoes and wall
501 paintings). Although SEM observation did not reveal the formation of a clear surface crust
502 in the present study, this possible issue is particularly important in the case of colored
503 plasters, so it will be further specifically investigated in the future.

504

505 REFERENCES

506 [1] Toniolo, L.; Paradisi, A.; Goidanich, S.; Pennati, G. Mechanical behaviour of lime based
507 mortars after surface consolidation *Constr. Build. Mater.* **2011**, *25*, 1553–1559, doi:
508 10.1016/j.conbuildmat.2010.08.010

509 [2] Giorgi, R.; Dei, L.; Baglioni, P. A New Method for Consolidating Wall Paintings Based on
510 Dispersions of Lime in Alcohol, *Stud. Conserv.* **2000**, *45*, 154-161,
511 doi:10.1179/sic.2000.45.3.154

512 [3] Ambrosi, M.; Dei, L.; Giorgi, R.; Neto, C.; Baglioni, P. Colloidal particles of Ca(OH)₂:
513 Properties and applications to restoration of frescoes, *Langmuir.* **2001**, *17*, 4251-4255,
514 doi:10.1021/la010269b

515 [4] Chelazzi, D.; Poggi, P.; Jaidar, Y.; Toccafondi, N.; Giorgi, R.; Baglioni, P. Hydroxide
516 nanoparticles for cultural heritage: Consolidation and protection of wall paintings and
517 carbonate materials *J. Colloid Interface Sci.* **2013**, *392*, 42–49, doi:10.1016/j.jcis.2012.09.069

518 [5] Arizzi, A.; Gomez-Villalba, L.S.; Lopez-Arce, P.; Cultrone, G.; Fort, R. Lime mortar
519 consolidation with nanostructured calcium hydroxide dispersions: the efficacy of different

- 520 consolidating products for heritage conservation. *Eur. J. Miner.* **2015**, *27*, 311-323,
521 doi:10.1127/ejm/2015/0027-2437
- 522 [6] Borsoi, G.; Lubelli, B.; van Hees, R.; Veiga, R.; Silva, A.S. Evaluation of the effectiveness
523 and compatibility of nanolime consolidants with improved properties. *Construct. Building*
524 *Mater.* **2017**, *142*, 385-394, doi:10.1016/j.conbuildmat.2017.03.097
- 525 [7] Delgado Rodrigues, J.; Ferreira Pinto, A.P.; Nogueira, R.; Gomes, A. Consolidation of lime
526 mortars with ethyl silicate, nanolime and barium hydroxide. Effectiveness assessment with
527 microdrilling data, *J. Cult. Herit.* **2018**, *29*, 43-53, doi:10.1016/j.culher.2017.07.006
- 528 [8] Otero, J.; Starinieri, V.; Charola, A.E.; Taglieri, G. Influence of different types of solvent on
529 the effectiveness of nanolime treatments on highly porous mortar substrates, *Constr. Build.*
530 *Mater.* **2020**, *230*, 117112, doi:10.1016/j.conbuildmat.2019.117112
- 531 [9] Delgado Rodrigues, J; Grossi, A. Indicators and ratings for the compatibility assessment of
532 conservation actions J. Cult. Herit. **2007**, *8*, 32–43, doi: 10.1016/j.culher.2006.04.007
- 533 [10] Balonis-Sant, M.; Ma, X.; Kakoulli, I. Preliminary results on biomimetic methods based on
534 soluble ammonium phosphate precursors for the consolidation of archaeological wall
535 paintings. In *Archaeological Chemistry VIII, ACS Symposium Series*; American Chemical
536 Society: Washington, DC, USA, **2013**; Volume 1147, pp. 419–447, doi:10.1021/bk-2013-
537 1147.ch022.
- 538 [11] Sassoni, E.; Franzoni, E. Lime and cement mortar consolidation by ammonium phosphate.
539 *Constr. Build. Mater.* **2020**, *245*, 118409, doi:10.1016/j.conbuildmat.2020.118409
- 540 [12] Masi, G.; Sassoni, E. Comparison between ammonium phosphate and nanolimes for render
541 consolidation, *IOP Conference Series: Materials Science and Engineering.* **2020**. ISSN:
542 1757-8981 vol. 949, p.1-8. doi:10.1088/1757-899X/949/1/012039
- 543 [13] Defus, A.; Possenti, E.; Sansonetti, A.; Tedeschi, C.; Colombo, C.; Biondelli, D.; Vettori, S.;
544 Realini, M. Di-ammonium hydrogen phosphate for the consolidation of lime-based historic
545 mortars – Preliminary research, *J. Cult. Herit.* **2021**, doi:10.1016/j.culher.2021.01.005
- 546 [14] Baglioni, P.; Carretti, E.; Chelazzi, D. Nanomaterials in art conservation. *Nat. Nanotechnol.*
547 **2015**, *10*, 287–290, doi: 10.1038/nnano.2015.38.
- 548 [15] Rodriguez-Navarro, C; Ruiz-Agudo, E. Nanolimes: from synthesis to application. *Pure Appl.*
549 *Chem.* **2018**, *90*, 523–550, doi: 10.1515/pac-2017-0506
- 550 [16] Ruffolo, S.A.; La Russa, M.F.; Ricca, M.; Belfiore, C.M.; Macchia, A.; Comite, V.; Pezzino, A.;
551 Crisci, G.M. New insights on the consolidation of salt weathered limestone: the case study of
552 Modica stone. *Bull. Eng. Geol. Environ.* **2017**, *76*, 11-20, doi:10.1007/s10064-015-0782-1
- 553 [17] Licchelli, M.; Malagodi, M.; Weththimuni, M.; Zanchi, C. Nanoparticles for conservation of
554 bio-calcareous stone, *Appl. Phys. A.* **2014**, *114*, 673-683. doi:10.1007/s00339-013-7973-z
- 555 [18] Ruffolo, S.A.; La Russa, M.F.; Aloise, P.; Belfiore, C.M.; Macchia, A.; Pezzino, A.; Crisci,
556 G.M. Efficacy of nanolime in restoration procedures of salt weathered limestone rock. *Appl.*
557 *Phys. A.* **2014**, *114*, 753–758, doi:10.1007/s00339-013-7982-y
- 558 [19] Sassoni, E.; Naidu, S.; Scherer, G.W. The use of hydroxyapatite as a new inorganic
559 consolidant for damaged carbonate stones. *J. Cult. Herit.* **2011**, *12*, 346–355,
560 doi:10.1016/j.culher.2011.02.005.
- 561 [20] Sassoni, E.; Hydroxyapatite and Other Calcium Phosphates for the Conservation of Cultural
562 Heritage: A Review. *Materials.* **2018**, *11*, 557, doi:10.3390/ma11040557
- 563 [21] Naidu, S.; Scherer, G.W. Nucleation, growth and evolution of calcium phosphate films on
564 calcite. *J. Colloid Interface Sci.* **2014**, *435*, 128–137, doi:10.1016/j.jcis.2014.08.018.
- 565 [22] Yang, F.; Zhang, B.; Liu, Y.; Wei, G.; Zhang, H.; Chen, W.; Xu, Z. Biomimic conservation of
566 weathered calcareous stones by apatite. *New J. Chem.* **2011**, *35*, 887–892,
567 doi:10.1039/c0nj00783h.
- 568 [23] Weththimuni, M.L.; Licchelli, M.; Malagodi, M.; Rovella, N.; La Russa, M. Consolidation of
569 bio-calcareous stone by treatment based on diammonium hydrogen phosphate and calcium

- 570 hydroxide nanoparticles. *Measurement*. **2018**, 127, 396–405, doi:
571 10.1016/j.measurement.2018.06.007
- 572 [24] Pesce, C.; Moretto, L.M.; Orsega, O.; Pesce, G.; Corradi, M.; Weber, J. Effectiveness and
573 compatibility of a novel sustainable method for stone consolidation based on di-ammonium
574 phosphate and calcium-based nanomaterials. *Materials*. **2019**, 12, 3025;
575 doi:10.3390/ma12183025
- 576 [25] Sassoni, E.; Graziani, G.; Franzoni, E. An innovative phosphate-based consolidant for
577 limestone. Part 2: Durability in comparison with ethyl silicate. *Construct. Build. Mater.* **2016**,
578 102, 931–942, doi:10.1016/j.conbuildmat.2015.10.202.
- 579 [26] Shekofteh, A.; Molina, E.; Rueda-Quero, L.; Arizzi, A.; Cultrone, G. The efficiency of
580 nanolime and dibasic ammonium phosphate in the consolidation of beige limestone from the
581 Pasargadae World Heritage Site. *Archaeol Anthropol Sci*, **2019**, doi:10.1007/s12520-019-
582 00863-y
- 583 [27] Sassoni, E.; Ugolotti, G.; Pagani M. Nanolime, nanosilica or ammonium phosphate?
584 Laboratory and field study on consolidation of a byzantine marble sarcophagus. *Construct.*
585 *Build. Mater.* **2020**, 262, 120784, doi:10.1016/j.conbuildmat.2020.120784
- 586 [28] Sassoni, E.; Mazzotti, C.; Pagliai, G. Comparison between experimental methods for
587 evaluating the compressive strength of existing masonry buildings, *Construct. Build. Mater.*
588 **2014**, 68, 206-219, DOI: 10.1016/j.conbuildmat.2014.06.070
- 589 [29] Sassoni, E.; Graziani, G.; Franzoni, E.; Scherer, G.W. Calcium phosphate coatings for
590 marble conservation: Influence of ethanol and isopropanol addition to the precipitation
591 medium on the coating microstructure and performance. *Corros. Sci.* **2018**, 136, 255–267,
592 doi:10.1016/j.corsci.2018.03.019.
- 593 [30] Sassoni, E.; Andreotti, S.; Scherer, G.W.; Franzoni, E.; Siegesmund S. Bowing of marble
594 slabs: can the phenomenon be arrested and prevented by inorganic treatments?,
595 *Environmental Earth Sciences*. **2018**, 77, 387, doi: 10.1007/s12665-018-7547-7
- 596 [31] Franzoni, E.; Sassoni, E.; Graziani, G. Brushing, poultice or immersion? The role of the
597 application technique on the performance of a novel hydroxyapatite-based consolidating
598 treatment for limestone. *J. Cult. Herit.* **2015**, 16, 173–184, doi:10.1016/j.culher.2014.05.009.
- 599 [32] European Standard EN 15801, Conservation of cultural property - Test methods -
600 Determination of water absorption by capillarity, **2010**
- 601 [33] Ruedrich, J., Knell, C., Enseleit, J., Rieffel, Y., Siegesmund, S.,. Stability assessment of
602 marble statues of the Schlossbrücke (Berlin, Germany) based on rock strength
603 measurements and ultrasonic wave velocities. *Environ Earth Sci.* **2013**, 69, 1451–1469, doi:
604 10.1007/s12665-013-2246-x.
- 605 [34] Drdäcký, M.; Lesàk, J.; Rescic, S.; Sližková, Z.; Tiano, P.; Valach, J. Standardization of
606 peeling tests for assessing the cohesion and consolidation characteristics of historic stone
607 surfaces, *Mater and Struct.* **2012**, 45, 505-520, doi: 10.1617/s11527-011-9778-x
- 608 [35] European Standard EN 12371, Natural stone test methods - Determination of frost
609 resistance, **2010**
- 610 [36] Karampas, I.A.; Kontoyannis, C.G. Characterization of calcium phosphates mixtures. *Vib*
611 *Spectrosc.* **2013**, 64, 126– 133, doi:10.1016/j.vibspec.2012.11.003
- 612 [37] Possenti, E.; Colombo, C.; Conti, C.; Gigli, L.; Merlini, M.; Rikkert Plaisier, J.; Realini, M.;
613 Sali, D.; Gatta, D. Diammonium hydrogenphosphate for the consolidation of building
614 materials. Investigation of newly-formed calcium phosphates. *Construct. Build. Mater.* **2019**,
615 195, 557–563, doi: 10.1016/j.conbuildmat.2018.11.077
- 616 [38] Possenti, E.; Conti, C.; Gatta, D.; Realini, M.; Colombo, C. Synchrotron radiation m X-ray
617 diffraction in transmission geometry for investigating the penetration depth of conservation
618 treatments on cultural heritage stone materials. *Anal. Methods*, **2020**, 12, 1587, doi:
619 10.1039/D0AY00010H

- 620 [39] Maravelaki-Kalaitzaki P. Black crusts and patinas on Pentelic marble from the Parthenon and
621 Erecteum (Acropolis, Athens): characterization and origin. *Anal. Chim. Acta.* **2005**, 532, 187–
622 98, doi: 10.1016/j.aca.2004.10.065
- 623 [40] Borsoi, G.; Lubelli, B.; van Hees, R.; Veiga, R.; Silva, A.S. Understanding the transport of
624 nanolime consolidants within Maastricht limestone. *J. Cult. Herit.* **2016**, 18, 242-249,
625 doi:10.1016/j.culher.2015.07.014
- 626 [41] Sharma, G. Color fundamentals for digital imaging. In *Digital Color Imaging Handbook*;
627 CRC Press: Boca Raton, FL, USA, **2003**.
- 628 [42] Rodrigues, J.D.; Grossi, A. Indicators and ratings for the compatibility assessment of
629 conservation actions. *J. Cult. Herit.* **2007**, 8, 32–43, doi:10.1016/j.culher.2006.04.007.
- 630 [43] Sassoni, E.; Graziani, G.; Franzoni, E. An innovative phosphate-based consolidant for
631 limestone. Part 1: Effectiveness and compatibility in comparison with ethyl silicate. *Construct.*
632 *Build. Mater.* **2016**, 102, 918–930, doi:10.1016/j.conbuildmat.2015.04.026.
- 633 [44] Scherer, G.W.; Wheeler, G.S. Silicate consolidants for stone. *Key Eng. Mater.* **2009**, 391, 1–
634 25, doi:10.4028/0-87849-365-4.1.